

Ultrahigh-Precision Hamiltonian Parameter Estimation in a Superconducting Circuit

Sai Li^{1,2,*}, De-Jian Pan^{1,*}, Yuan-Ke Zhu^{1,*}, Jia-Lang Zhou¹, Wen-Cui Liao¹, Wei-Xin Zhang¹, Zhen-Tao Liang^{1,2}, Qing-Xian Lv^{1,2}, Haifeng Yu^{3,4}, Zheng-Yuan Xue^{1,2,4,†}, Hui Yan^{1,2,4,‡} and Shi-Liang Zhu^{1,2,4,§}

¹Key Laboratory of Atomic and Subatomic Structure and Quantum Control (Ministry of Education), Guangdong Basic Research Center of Excellence for Structure and Fundamental Interactions of Matter, and School of Physics, South China Normal University, Guangzhou 510006, China

²Guangdong Provincial Key Laboratory of Quantum Engineering and Quantum Materials, Guangdong-Hong Kong Joint Laboratory of Quantum Matter, and Frontier Research Institute for Physics, South China Normal University, Guangzhou 510006, China

³Beijing Academy of Quantum Information Sciences, Beijing 100193, China

⁴Hefei National Laboratory, Hefei 230088, China



(Received 22 March 2024; accepted 21 May 2024; published 18 June 2024)

The Hamiltonian, which determines the evolution of a quantum system, is fundamental in quantum physics. Therefore, it is crucial to implement high-precision generation and measurement of the Hamiltonian in a practical quantum system. Here, we experimentally demonstrate ultrahigh-precision Hamiltonian parameter estimation with a significant quantum advantage in a superconducting circuit via sequential control. We first observe the commutation relation for noncommuting operations determined by the system Hamiltonian, both with and without adding quantum control, verifying the commuting property of controlled noncommuting operations. Based on this control-induced commuting property, we further demonstrate Hamiltonian parameter estimation for polar and azimuth angles in superconducting circuits, achieving ultrahigh metrological gains in measurement precision exceeding the standard quantum limit by up to 16.0 and 16.1 dB at $N = 100$, respectively.

DOI: [10.1103/PhysRevLett.132.250204](https://doi.org/10.1103/PhysRevLett.132.250204)

Quantum systems possess magical and fascinating properties [1–4], such as quantum superposition, quantum entanglement, and quantum non-clonability, which provide basic principles for the field of quantum information. Significant progress has been made to promote the development of various quantum information technologies [5–7]. Quantum metrology [8–12], which utilizes quantum resources such as quantum entanglement and coherence, can achieve higher precision of measurements beyond the standard quantum limit (SQL) and reaching the Heisenberg limit (HL) [13–16], which is constrained by the Heisenberg uncertainty principle [17].

The enhanced precision of measurements in quantum metrology holds promising applications in various fields of modern physics, such as atomic clocks [18], spectroscopy [19,20], magnetometry [21,22], gravitational wave detection [23], dark matter detection [24], etc. Thus, extensive efforts have been dedicated to improving the measurement precision. A direct way of this improvement can be achieved by preparing the probe as entangled states [14,25–32]. However, as the number of particles in entangled states increases, the difficulty of their preparation and manipulation will dramatically escalate, and thus posing significant obstacles for their practical applications in quantum metrology.

Alternatively, a single quantum mode without entanglement has been explored to realize quantum metrological advantages using nonclassical bosonic states [33,34], such

as number states [35,36] and superposition of Fock states with maximum variance [37,38]. Although quantum metrological advantages with nonclassical bosonic states have been demonstrated, the metrological gains are still limited by the experimentally achievable photon numbers. Instead of exploring high photon number states in a single bosonic mode or the number of particles in entangled states, direct sequential (or multi-round) protocol [9,15,39,40] can also achieve the HL. This protocol utilizes the coherence from sequential evolution of a single probe as the quantum resource, and thus greatly decreases the complexity of quantum manipulations.

Hamiltonian parameter estimation (HPE) is essential for quantum information as it is the basis of precise quantum control. With the direct sequential protocol, HPE under sequential commuting quantum dynamics is directly realizable experimentally [15,40]. Meanwhile, in the case of HPE under noncommuting quantum dynamics [41], by adding quantum control, it can be transformed into effective commuting ones [42,43], thereby experimentally achieving the HL in optical systems [44,45]. However, optical systems can only simulate the evolution process and cannot directly generate the Hamiltonian itself. Additionally, due to the limitation of experimental implementation in optical systems, HPE has only been demonstrated in a small sequential round with less metrological gains [44,45], lacking for demonstration of stronger quantum metrological advantage.

In this Letter, we experimentally demonstrate ultrahigh-precision HPE under noncommuting dynamics in a superconducting transmon qubit via sequential control. Transmon qubits [46–50] have the merits of long coherence time, simple microwave control and high-fidelity readout, thus providing an excellent platform for high-precision measurement. The commuting property of the evolution operator at different parameters is essential for achieving HL quantum metrology with sequential control. We experimentally demonstrate that the commuting property can be achieved through the addition of designed controls for noncommuting operations. We then implement repeated controlled noncommuting dynamics for sensing polar and azimuth angles in the system Hamiltonian, demonstrating remarkable metrological gains surpassing the SQL by up to 16.0 and 16.1 dB at $N = 100$ times of repeated dynamics, respectively. We also demonstrate with numerical calculations the superiority of our controlled parallel protocol compared to the traditional parallel methods employing multiparticle entanglement. Our work demonstrates stronger quantum advantages for HPE, and thus opens a new avenue for superconducting circuits in the field of quantum metrology.

We first introduce the HPE schemes. We assume a generic Hamiltonian $H(p)$ of a quantum system with a specific parameter p and the aim is to find an optimal method to precisely measure p . For N individual measurements, the optimal variance δp is limited by the standard quantum limit, i.e., $\delta p = \eta_S / \sqrt{N}$, with η_S a constant. However, benefits from the quantum advantages of quantum resources, such as quantum entanglement or quantum coherence, one can go beyond the SQL to the HL which is described by $\delta p = \eta_H / N$, with η_H a constant [7,12]. To achieve HL for HPE, as shown in Fig. 1(a), one can utilize parallel protocol which entangles multicopy of the systems [25–29], and then each copy evolves with an evolution operator $U(p) = e^{-iH(p)T}$ governed by the Hamiltonian $H(p)$ through a time interval of T . The precision of this measurement can approach the HL based on the advantages of the entangled state. Alternatively, If the evolution operator satisfies commutator $[U(p), U(p')] = 0$, the sequential protocol shown in Fig. 1(b) can also achieve the HL. Unlike the parallel protocol, the sequential protocol [9] converts the way of parallel operations on the entangled state into repeated operations on a probe state.

However, for noncommuting dynamics with commutator $[U(p), U(p')] \neq 0$ at different values of the parameter p , it cannot directly achieve the HL for sensing parameter p [41]. Notably, as depicted in Fig. 1(c), we demonstrate that reaching the HL is feasible if a quantum control operator C can be identified to transform the noncommuting dynamics into the paired commuting dynamics for different values of p [42]. Specifically, this transformation is characterized by the following condition:

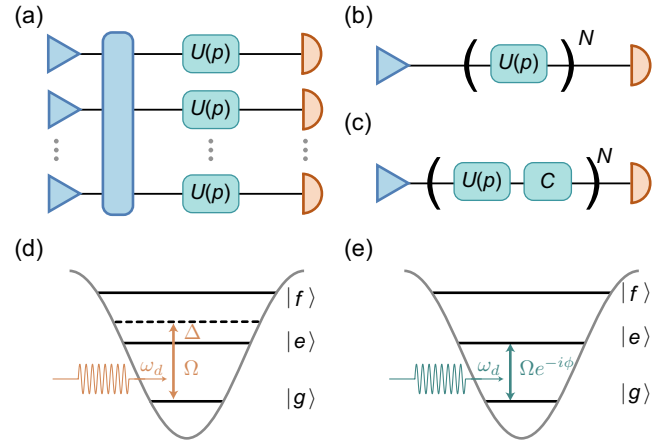


FIG. 1. Schematic illustration of HPE for approaching the HL. (a) Parallel protocol for HPE of a parameter p involving an N -particles entangled state, N same parallel unitary operators $U(p)$, and separable measurements. (b) Sequential protocol for HPE involving an input state, N same sequential unitary operators $U(p)$, and a measurement. Both parallel protocol and sequential protocol are only suitable for HPE under commuting dynamics at different values of p . (c) Controlled sequential protocol for HPE involving an input state, N same sequential operators $U(p)$ and control operators C , and a measurement. The controlled sequential protocol can transform the noncommuting dynamics into commuting ones. (d) and (e) Energy level diagrams of a superconducting transmon qubit driven by an off-resonant and a resonant square microwave pulse on the transition of $|g\rangle \leftrightarrow |e\rangle$, respectively. These drives individually generate the Hamiltonian $H(\theta)$ (d) and $H(\phi)$ (e).

$$[CU(p), CU(p')] = 0. \quad (1)$$

In this scenario, the additional control is uniform for all parameter values of p , eliminating the need for adaptive updating. To illustrate, we consider a qubit system as an example, where controlled noncommuting dynamics can be expressed as $\mathcal{O}(p) \equiv CU(p) = \exp(-ip\Lambda \cdot \sigma)$, where $\Lambda \cdot \sigma$ denotes as a p -independent rotation axis with $\Lambda = (\Lambda_x, \Lambda_y, \Lambda_z)$ and Pauli matrices $\sigma = (\sigma_x, \sigma_y, \sigma_z)$, then control-induced sequential paired commuting dynamics are described by $\mathcal{O}_N(p) = [CU(p)]^N = \exp(-iNp\Lambda \cdot \sigma)$.

To obtain the HL for HPE of the controlled sequential dynamics $\mathcal{O}_N(p)$, we introduce $G_p = i[\partial_p \mathcal{O}(p)]\mathcal{O}^\dagger(p)$ as the generator of parameter translation with respect to p . For a pure initial state $|\psi\rangle$, the quantum Fisher information (QFI) [41,51] of the evolved state $|\zeta\rangle = \mathcal{O}_N(p)|\psi\rangle$ is given by

$$\mathcal{F} = 4\langle \zeta | \Delta G_p^2 | \zeta \rangle. \quad (2)$$

When optimal probe states and measurements are chosen, the QFI can reach its maximal value as

$$\mathcal{F}_{\max} = [\lambda_{\max}(G_p) - \lambda_{\min}(G_p)]^2, \quad (3)$$

where $\lambda_{\max}(G_p)$ and $\lambda_{\min}(G_p)$ are maximal and minimal eigenvalues of G_p , respectively. Here, we set the generator as $G_p = N\mathbf{\Lambda} \cdot \boldsymbol{\sigma}$ with $\lambda_{\max}(G_p) = N|\mathbf{\Lambda}|$ and $\lambda_{\min}(G_p) = -N|\mathbf{\Lambda}|$. Then, we can obtain the maximal QFI $\mathcal{F}_{\max} = 4(N|\mathbf{\Lambda}|)^2$ and measurement precision $\delta p = 1/(2N|\mathbf{\Lambda}|)$, reaching the HL.

We experimentally realize this protocol with a superconducting transmon qubit [49], defined by the lowest two levels $\{|g\rangle, |e\rangle\}$ with frequency $\omega = 4.686$ GHz and coherence time $T_1 = 76$ μ s. More details of the device parameters can be found in Ref. [52]. To generate the system Hamiltonian, we apply a detuned square microwave pulse $\Omega \cos \omega_d t$ on the qubit, as shown in Fig. 1(d), where Ω and ω_d are the amplitude and frequency of the pulse, respectively. In the interaction picture, the Hamiltonian is described by a spin-half particle subject to an effective magnetic field, i.e.,

$$H_1(\theta)/\hbar = J(\cos \theta \sigma_z + \sin \theta \sigma_x), \quad (4)$$

where $J = \sqrt{(\Omega^2 + \Delta^2)}/2$ is an effective coupling strength, with $\Delta = \omega - \omega_d$, and $\theta = \arctan(\Omega/\Delta)$ denotes as polar angle on the parameter space determined by the effective magnetic field. To achieve the HL in estimating θ , a control operation $C \equiv Z = \sigma_z$ is added at the time $JT = \pi/2$. Then, the total controlled evolution operator is $ZU_1(\theta) = \sigma_z \exp[-i(\pi/2)(\cos \theta \sigma_z + \sin \theta \sigma_x)] = -i \exp(i\theta \sigma_y)$, representing a rotation around the axis σ_y , which satisfies the commutation relation in Eq. (1) for all polar angles θ . As shown in Ref. [52], the QFI can reach $4N^2$, leading to a HL $\delta\theta = 1/2N$ for estimating the polar angle. In our experiment, the time $T = 400$ ns is set to decrease the influence of microwave pulse induced stark shift due to the limited anharmonicity of the qubit. The amplitude Ω is accurately calibrated by the direct sequential protocol at the time $T = 400$ ns and $\theta = \pi/2$ to mitigate its influence on HPE [52]. The Z operation is realized by a virtual- Z gate, consuming no time resources.

In addition, as shown in Fig. 1(e), when a square microwave pulse with an amplitude Ω and a phase ϕ is resonantly applied on the qubit, the Hamiltonian in the interaction picture can be written, in the basis of $\{|g\rangle, |e\rangle\}$, as

$$H_2(\phi)/\hbar = \frac{\Omega}{2}(\cos \phi \sigma_x + \sin \phi \sigma_y), \quad (5)$$

where ϕ denotes as azimuth angle on the parameter space. To achieve the HL in estimating ϕ , a control operation $C \equiv X = \sigma_x$ is added at the time $\Omega T = \pi$ with $T = 400$ ns. Then, the total controlled evolution operator is $XU_2(\phi) = \sigma_x \exp[-i(\pi/2)(\cos \phi \sigma_x + \sin \phi \sigma_y)] = -i \exp(i\phi \sigma_z)$, representing a rotation around the σ_z axis, which also meets the commutation relation in Eq. (1) for all azimuth angles ϕ . As shown in Ref. [52], the QFI can reach $4N^2$, achieving a HL $\delta\phi = 1/(2N)$ for estimating the azimuth angle. In our experiment,

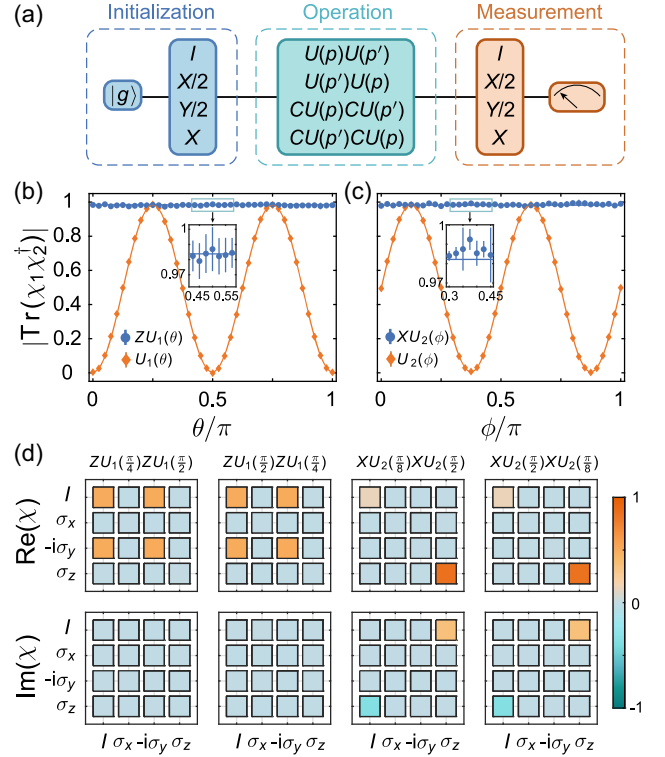


FIG. 2. Observation of the commutation relation. (a) Experimental sequence to perform the QPT for the operations in the commutation relation for noncommuting operations with and without control. (b) and (c) Measured values $|\text{Tr}(\chi_1 \chi_2^\dagger)|$ for the quantification of commutation relation of $[ZU_1(\pi/4), ZU_1(\theta)]$, $[U_1(\pi/4), U_1(\theta)]$, $[XU_2(\pi/8), XU_2(\phi)]$, and $[U_2(\pi/8), U_2(\phi)]$ with χ_1 and χ_2 as the quantum process matrix of operations $\mathcal{P}\mathcal{Q}$ and $\mathcal{Q}\mathcal{P}$ in the commutation relation of $[\mathcal{P}, \mathcal{Q}]$, respectively. Error bars, obtained from 5 repeated experiments, are smaller than the marker sizes. Solid lines are from numerical simulations. The insets in (b) and (c) are enlarged plots for each case. (d) The real and imaginary parts of the measured quantum process matrices χ of the four quantum operations $ZU_1(\pi/4)ZU_1(\pi/2)$, $ZU_1(\pi/2)ZU_1(\pi/4)$, $XU_2(\pi/8)XU_2(\pi/2)$, and $XU_2(\pi/2)XU_2(\pi/8)$. The color bar represents the magnitude of the real and imaginary parts of the quantum process matrices with dimensionless unit.

the X operation is generated by a π pulse, which has a cosine-shaped envelope with a duration of 50 ns. Additionally, the technique of “derivative removal by adiabatic gate” [57,58] is applied to suppress the leakage to higher energy levels.

In our experiment, we first verify the commutation relation for noncommuting operations with and without adding quantum control using quantum process tomography (QPT) [59], with the experimental sequence shown in Fig. 2(a). The quantification of the commutation relation of $[\mathcal{P}, \mathcal{Q}]$ is transformed into the value of $|\text{Tr}(\chi_1 \chi_2^\dagger)|$, where Tr represents the trace, χ_1 and χ_2 are the quantum process matrix of operations $\mathcal{P}\mathcal{Q}$ and $\mathcal{Q}\mathcal{P}$, respectively. Figures 2(b) and 2(c) show the values of the commutation relation of $[ZU_1(\pi/4), ZU_1(\theta)]$,

$[U_1(\pi/4), U_1(\theta)]$, $[XU_2(\pi/8), XU_2(\phi)]$, and $[U_2(\pi/8), U_2(\phi)]$, respectively. For the case of the noncommuting operations with adding quantum control, all values of the commutation relation are close to 1, implying that the noncommuting operations with quantum control have been transformed into commuting one. Furthermore, the measured process matrices for $ZU_1(\pi/4)ZU_1(\pi/2)$, $ZU_1(\pi/2)ZU_1(\pi/4)$, $XU_2(\pi/8)XU_2(\pi/2)$, and $XU_2(\pi/2)XU_2(\pi/8)$ are presented, respectively, in Fig. 2(d). Verification of the commuting property for controlled noncommuting dynamics enables the implementation of HPE for noncommuting dynamics. Furthermore, the performance of noncommuting dynamics with and without quantum control is characterized by both QPT and the cross-entropy benchmarking method [60,61], with experimental results showing high fidelity [52], which allows for multiround controlled noncommuting dynamics.

To demonstrate ultrahigh-precision HPE for the polar angle θ , we perform experiments under sequential noncommuting dynamics with N quantum controls and showcase the advantages beyond the SQL. The experimental sequence is depicted in Fig. 3(a), where the optimal probe state is prepared as $|\psi\rangle = |g\rangle$, the control operation $Z = \sigma_z$ is added after the evolution operator $U_1(\theta) = \exp[-iH(\theta)T]$, and the optimal measurement is the projective measurement on the eigenvector of σ_x . The ideal probabilities of the measurement outcomes are $P_{\text{id}}^N = (1 + \sin 2N\theta)/2$. The experimental measurement results of the probability distributions P_{exp}^N with $N = 1, 5, 10, 20$ as examples at different polar angles $\theta \in [0, \pi]$ are shown in Fig. 3(b). Because of the decoherence of the qubit, the oscillation contrast of the measured interference fringes gradually decreases as the number N of quantum controls increasing, which can be fitted by the function $P^N = (1 + A \sin 2N\theta)/2$, where A represents the oscillation contrast. Then, the measurement precision can be inferred as $\delta\theta = \sqrt{P^N(1-P^N)}/(dP^N/d\theta) = 1/(2NA)$ [13]. Figure 3(c) shows the results of $\delta\theta$ as a function of N in a logarithmic-logarithmic scale. The results demonstrate that the polar angle sensing beats the SQL, surpassing the SQL with a maximum metrological gain of $20 \log(\delta\theta_{\text{SQL}}/\delta\theta) = 16.0$ dB at $N = 100$. Additionally, the obtained precision scales as $N^{-0.93}$ for $N \leq 100$, approaching the Heisenberg scaling of N^{-1} . The difference is mainly caused by the decoherence effect of the qubit [52], limiting greater metrological gain, which can be further enhanced by shortening the evolution time T and/or improving the coherence of the qubit.

For HPE of the azimuth angle ϕ , we perform experiments with sequence depicted in Fig. 4(a). The optimal probe state is first prepared as $|\psi\rangle = (|g\rangle - i|e\rangle)/\sqrt{2}$, then the quantum control operation $X = \sigma_x$ is added after the evolution operator $U_2(\phi) = \exp[-iH(\phi)T]$, and the optimal measurement is the projective measurement on the

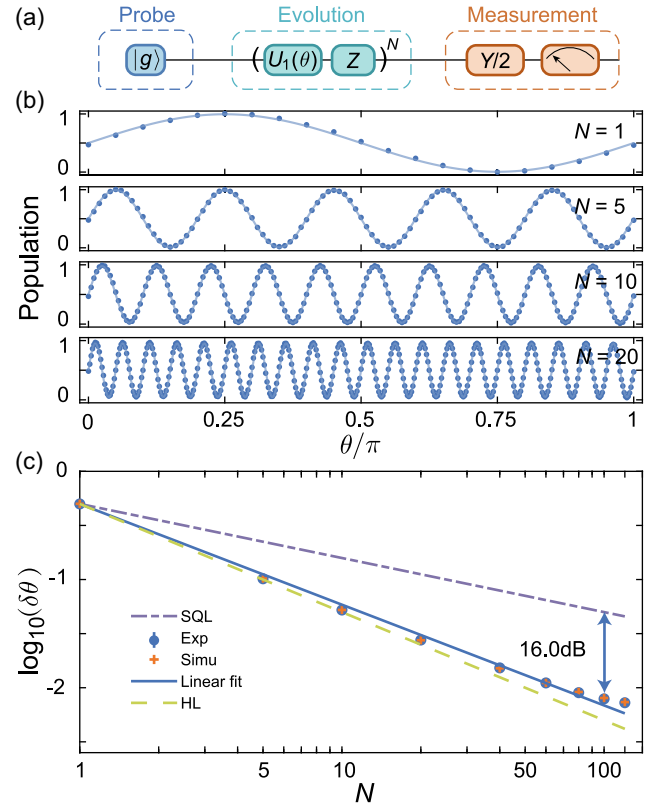


FIG. 3. Experimental HPE for the polar angle θ . (a) Quantum circuit for sensing θ in the system Hamiltonian. (b) Measured qubit ground state populations (dots) and corresponding fittings (solid lines) as a function of θ under N controlled dynamics, with $N = 1, 5, 10, 20$ as examples. Error bars, obtained from 5 repeated experiments, are smaller than the marker sizes. (c) Measurement precision $\delta\theta$ as a function of the number of N controls. The blue dots are experimental results with error bars obtained by the standard deviations of A in fitting the data in (b), which are smaller than the marker sizes. A metrological gain of 16.0 dB surpassing the SQL (purple dashed line) is achieved at $N = 100$. The solid blue line is a linear fit, giving a precision scaling of $N^{-0.93}$, approaching the Heisenberg scaling N^{-1} (yellow dashed line). The red crosses are the results obtained from numerical simulations that include the decoherence and anharmonicity of the qubit, showing good agreement with the experimental results.

eigenvector of σ_x . Consequently, this azimuth angle sensing yields a similar oscillation curve as a function of the azimuth angle ϕ , as shown in Fig. 4(b). The resulting azimuth angle sensing beats the SQL as well, as depicted in Fig. 4(c), with a maximum metrological gain of 16.1 dB at $N = 100$ and a precision scaling of $N^{-0.93}$ for $N \leq 100$, approaching the Heisenberg scaling.

Furthermore, we showcase the quantum metrological superiority of the demonstrated controlled sequential protocol by comparing it with the controlled parallel protocol [52]. The parallel protocol requires the optimal probe state to be prepared on a multiparticle entangled state, e.g., the Greenberger-Horne-Zeilinger (GHZ) state.

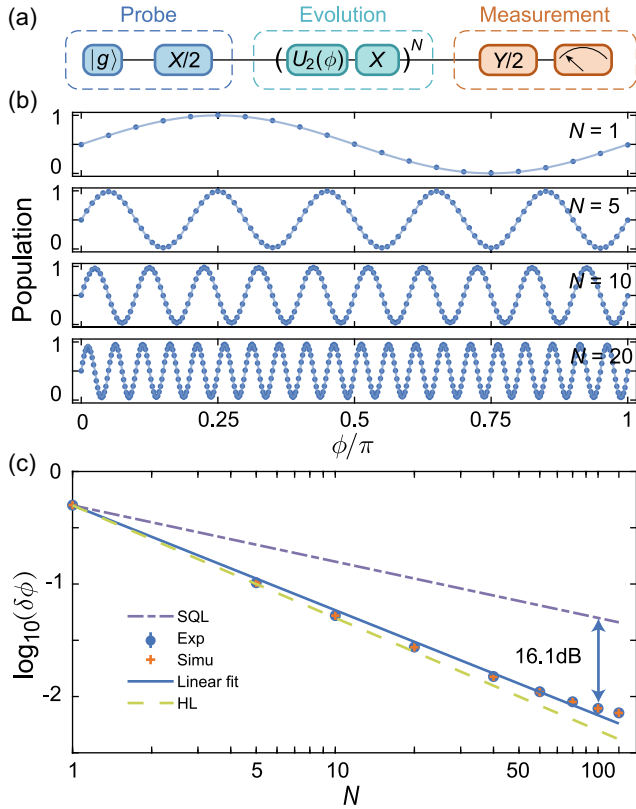


FIG. 4. Experimental HPE for the azimuth angle ϕ . (a) Quantum circuit for sensing ϕ . (b) The measured qubit ground state populations (dots) and corresponding fittings (solid lines) as a function of ϕ . (c) The measurement precision $\delta\phi$ as a function of the number of N quantum controls. The legends are the same as those in Fig. 3.

However, scalable generation of GHZ states on superconducting circuits is challenging [62], which demands precise quantum gates and reliable verification techniques. Thus, the current largest experimentally realized GHZ state in superconducting circuits is 18 qubits [28,29], which is significantly smaller than the capacity of the demonstrated controlled sequential method. Besides, the coherence of GHZ states degrades rapidly, following an N^2 scaling law [26], which limits the efficiency of the parallel protocol in metrological applications. Therefore, the enhanced efficiency of the controlled sequential protocol to quantum metrology has clear advantage over that of the controlled parallel protocol [52].

To summarize, we have experimentally demonstrated ultrahigh-precision HPE approaching the HL using a superconducting transmon qubit, employing a simple and hardware-efficient sequential control protocol. The commuting property for noncommuting operations with adding quantum control is verified, which is essential for HPE under noncommuting dynamics. Notably, our results have demonstrated remarkable metrological gains of 16.0 and 16.1 dB for the polar and azimuth angle sensing at $N = 100$, respectively. Furthermore, higher metrological

gain is possible with N rounds exceeding one thousand using a superconducting qubit, by prolonging its coherence time and enhancing the fidelity of operations [50]. Besides, numerical results show enhanced efficiency of the presented approach to quantum metrology over parallel methods employing multiparticle entanglement [52]. Additionally, quantum multiparameter estimation far surpassing the SQL at the same time [43,45] can be implemented by using two entangled superconducting qubits [49]. Our results indicate that superconducting circuits are appealing for HPE, further validating the controlled sequential protocol in the practical application of quantum metrology.

We thank Yang Yu and Yuan Xu for helpful discussions. This work was supported by the National Natural Science Foundation of China (Grants No. 12225405, No. U20A2074, No. 12275090, No. 12104168, No. 12304287, No. 12304554, No. 92365206, and No. 12074180), the Innovation Program for Quantum Science and Technology (Grant No. 2021ZD0301700), the National Key Research and Development Program of China (Grant No. 2022YFA1405300), the Project funded by China Postdoctoral Science Foundation (Grant No. 2023M741240), and Guangdong Provincial Quantum Science Strategic Initiative (Grant No. GDZX2304002).

*These authors contributed equally to this work.

†zyxue83@163.com

‡yanhui@scnu.edu.cn

§slzhu@scnu.edu.cn

- [1] P. A. M. Dirac, *The Principles of Quantum Mechanics: 4th ed.* (Oxford University Press, New York, 1958).
- [2] W. K. Wootters and W. H. Zurek, A single quantum cannot be cloned, *Nature (London)* **299**, 802 (1982).
- [3] A. Zeilinger, Experiment and the foundations of quantum physics, *Rev. Mod. Phys.* **71**, S288 (1999).
- [4] R. Horodecki, P. Horodecki, M. Horodecki, and K. Horodecki, Quantum entanglement, *Rev. Mod. Phys.* **81**, 865 (2009).
- [5] N. Gisin and R. Thew, Quantum communication, *Nat. Photonics* **1**, 165 (2007).
- [6] D. P. DiVincenzo, Quantum computation, *Science* **270**, 255 (1995).
- [7] C. L. Degen, F. Reinhard, and P. Cappellaro, Quantum sensing, *Rev. Mod. Phys.* **89**, 035002 (2017).
- [8] V. Giovannetti, S. Lloyd, and L. Maccone, Quantum-enhanced measurements: Beating the standard quantum limit, *Science* **306**, 1330 (2004).
- [9] V. Giovannetti, S. Lloyd, and L. Maccone, Quantum metrology, *Phys. Rev. Lett.* **96**, 010401 (2006).
- [10] V. Giovannetti, S. Lloyd, and L. Maccone, Advances in quantum metrology, *Nat. Photonics* **5**, 222 (2011).
- [11] H. Yuan and C.-H. F. Fung, Quantum parameter estimation with general dynamics, *npj Quantum Inf.* **3**, 14 (2017).

- [12] D. Braun, G. Adesso, F. Benatti, R. Floreanini, U. Marzolino, M. W. Mitchell, and S. Pirandola, Quantum-enhanced measurements without entanglement, *Rev. Mod. Phys.* **90**, 035006 (2018).
- [13] S. L. Braunstein and C. M. Caves, Statistical distance and the geometry of quantum states, *Phys. Rev. Lett.* **72**, 3439 (1994).
- [14] T. Nagata, R. Okamoto, J. L. O'Brien, K. Sasaki, and S. Takeuchi, Beating the standard quantum limit with four-entangled photons, *Science* **316**, 726 (2007).
- [15] B. L. Higgins, D. W. Berry, S. D. Bartlett, H. M. Wiseman, and G. J. Pryde, Entanglement-free Heisenberg-limited phase estimation, *Nature (London)* **450**, 393 (2007).
- [16] R. Demkowicz-Dobrzański and L. Maccone, Using entanglement against noise in quantum metrology, *Phys. Rev. Lett.* **113**, 250801 (2014).
- [17] W. Heisenberg, Über den anschaulichen inhalt der quantentheoretischen kinematik und mechanik, *Z. Phys.* **43**, 172 (1927).
- [18] L. Pezzè, A. Smerzi, M. K. Oberthaler, R. Schmied, and P. Treutlein, Quantum metrology with nonclassical states of atomic ensembles, *Rev. Mod. Phys.* **90**, 035005 (2018).
- [19] D. Leibfried, M. D. Barrett, T. Schaetz, J. Britton, J. Chiaverini, W. M. Itano, J. D. Jost, C. Langer, and D. J. Wineland, Toward Heisenberg-limited spectroscopy with multiparticle entangled states, *Science* **304**, 1476 (2004).
- [20] P. O. Schmidt, T. Rosenband, C. Langer, W. M. Itano, J. C. Bergquist, and D. J. Wineland, Spectroscopy using quantum logic, *Science* **309**, 749 (2005).
- [21] M. Koschorreck, M. Napolitano, B. Dubost, and M. W. Mitchell, Sub-projection-noise sensitivity in broadband atomic magnetometry, *Phys. Rev. Lett.* **104**, 093602 (2010).
- [22] J. B. Brask, R. Chaves, and J. Kołodyński, Improved quantum magnetometry beyond the standard quantum limit, *Phys. Rev. X* **5**, 031010 (2015).
- [23] R. X. Adhikari, Gravitational radiation detection with laser interferometry, *Rev. Mod. Phys.* **86**, 121 (2014).
- [24] N. Du, N. Force, R. Khatiwada, E. Lentz, R. Ottens, L. J. Rosenberg, G. Rybka, G. Carosi, N. Woollett, D. Bowring *et al.*, Search for invisible axion dark matter with the axion dark matter experiment, *Phys. Rev. Lett.* **120**, 151301 (2018).
- [25] W.-B. Gao, C.-Y. Lu, X.-C. Yao, P. Xu, O. Gühne, A. Goebel, Y.-A. Chen, C.-Z. Peng, Z.-B. Chen, and J.-W. Pan, Experimental demonstration of a hyper-entangled ten-qubit Schrödinger cat state, *Nat. Phys.* **6**, 331 (2010).
- [26] T. Monz, P. Schindler, J. T. Barreiro, M. Chwalla, D. Nigg, W. A. Coish, M. Harlander, W. Hänsel, M. Hennrich, and R. Blatt, 14-qubit entanglement: Creation and coherence, *Phys. Rev. Lett.* **106**, 130506 (2011).
- [27] A. Omran, H. Levine, A. Keesling, G. Semeghini, T. T. Wang, S. Ebadi, H. Bernien, A. S. Zibrov, H. Pichler, S. Choi, J. Cui, M. Rossignolo, P. Rembold, S. Montangero, T. Calarco, M. Endres, M. Greiner, V. Vuletić, and M. D. Lukin, Generation and manipulation of Schrödinger cat states in Rydberg atom arrays, *Science* **365**, 570 (2019).
- [28] C. Song, K. Xu, H. Li, Y.-R. Zhang, X. Zhang, W. Liu, Q. Guo, Z. Wang, W. Ren, J. Hao, H. Feng, H. Fan, D. Zheng, D.-W. Wang, H. Wang, and S.-Y. Zhu, Generation of multicomponent atomic Schrödinger cat states of up to 20 qubits, *Science* **365**, 574 (2019).
- [29] K. X. Wei, I. Lauer, S. Srinivasan, N. Sundaresan, D. T. McClure, D. Toyli, D. C. McKay, J. M. Gambetta, and S. Sheldon, Verifying multipartite entangled Greenberger-Horne-Zeilinger states via multiple quantum coherences, *Phys. Rev. A* **101**, 032343 (2020).
- [30] I. Afek, O. Ambar, and Yaron Silberberg, High-NOON states by mixing quantum and classical light, *Science* **328**, 879 (2010).
- [31] Y.-A. Chen, X.-H. Bao, Z.-S. Yuan, S. Chen, B. Zhao, and J.-W. Pan, Heralded generation of an atomic NOON state, *Phys. Rev. Lett.* **104**, 043601 (2010).
- [32] J. Zhang, M. Um, D. Lv, J.-N. Zhang, L.-M. Duan, and K. Kim, NOON states of nine quantized vibrations in two radial modes of a trapped ion, *Phys. Rev. Lett.* **121**, 160502 (2018).
- [33] A. Luis, Phase-shift amplification for precision measurements without nonclassical states, *Phys. Rev. A* **65**, 025802 (2002).
- [34] K. Duivenvoorden, B. M. Terhal, and D. Weigand, Single-mode displacement sensor, *Phys. Rev. A* **95**, 012305 (2017).
- [35] F. Wolf, C. Shi, J. C. Heip, M. Gessner, L. Pezzè, A. Smerzi, M. Schulte, K. Hammerer, and P. O. Schmidt, Motional Fock states for quantum-enhanced amplitude and phase measurements with trapped ions, *Nat. Commun.* **10**, 2929 (2019).
- [36] X. Deng, S. Li, Z.-J. Chen, Z. Ni, Y. Cai, J. Mai, L. Zhang, P. Zheng, H. Yu, C.-L. Zou, S. Liu, F. Yan, Y. Xu, and D. Yu, Heisenberg-limited quantum metrology using 100-photon fock states, [arXiv:2306.16919](https://arxiv.org/abs/2306.16919).
- [37] W. Wang, Y. Wu, Y. Ma, W. Cai, L. Hu, X. Mu, Y. Xu, Z.-J. Chen, H. Wang, Y. P. Song, H. Yuan, C.-L. Zou, L.-M. Duan, and L. Sun, Heisenberg-limited single-mode quantum metrology in a superconducting circuit, *Nat. Commun.* **10**, 4382 (2019).
- [38] K. C. McCormick, J. Keller, S. C. Burd, D. J. Wineland, A. C. Wilson, and D. Leibfried, Quantum-enhanced sensing of a single-ion mechanical oscillator, *Nature (London)* **572**, 86 (2019).
- [39] D. W. Berry, B. L. Higgins, S. D. Bartlett, M. W. Mitchell, G. J. Pryde, and H. M. Wiseman, How to perform the most accurate possible phase measurements, *Phys. Rev. A* **80**, 052114 (2009).
- [40] T. Juffmann, B. B. Klopfer, T. L. Frankort, P. Haslinger, and M. A. Kasevich, Multi-pass microscopy, *Nat. Commun.* **7**, 12858 (2016).
- [41] S. Pang and T. A. Brun, Quantum metrology for a general Hamiltonian parameter, *Phys. Rev. A* **90**, 022117 (2014).
- [42] H. Yuan and C.-H. F. Fung, Optimal feedback scheme and universal time scaling for Hamiltonian parameter estimation, *Phys. Rev. Lett.* **115**, 110401 (2015).
- [43] H. Yuan, Sequential feedback scheme outperforms the parallel scheme for Hamiltonian parameter estimation, *Phys. Rev. Lett.* **117**, 160801 (2016).
- [44] Z. Hou, R.-J. Wang, J.-F. Tang, H. Yuan, G.-Y. Xiang, C.-F. Li, and G.-C. Guo, Control-enhanced sequential scheme for general quantum parameter estimation at the Heisenberg limit, *Phys. Rev. Lett.* **123**, 040501 (2019).

- [45] Z. Hou, J.-F. Tang, H. Chen, H. Yuan, G.-Y. Xiang, C.-F. Li, and G.-C. Guo, Zero-trade-off multiparameter quantum estimation via simultaneously saturating multiple Heisenberg uncertainty relations, *Sci. Adv.* **7**, eabd2986 (2021).
- [46] J. Koch, T. M. Yu, J. Gambetta, A. A. Houck, D. I. Schuster, J. Majer, A. Blais, M. H. Devoret, S. M. Girvin, and R. J. Schoelkopf, Charge-insensitive qubit design derived from the Cooper pair box, *Phys. Rev. A* **76**, 042319 (2007).
- [47] H. Paik, D. I. Schuster, L. S. Bishop, G. Kirchmair, G. Catelani, A. P. Sears, B. R. Johnson, M. J. Reagor, L. Frunzio, L. I. Glazman, S. M. Girvin, M. H. Devoret, and R. J. Schoelkopf, Observation of high coherence in Josephson junction qubits measured in a three-dimensional circuit QED architecture, *Phys. Rev. Lett.* **107**, 240501 (2011).
- [48] A. P. M. Place, L. V. H. Rodgers, P. Mundada, B. M. Smitham, M. Fitzpatrick, Z. Leng, A. Premkumar, A. Bryon, Jacob adn Vrajitoarea, S. Sussman *et al.*, New material platform for superconducting transmon qubits with coherence times exceeding 0.3 milliseconds, *Nat. Commun.* **12**, 1779 (2021).
- [49] A. Blais, A. L. Grimsmo, S. M. Girvin, and A. Wallraff, Circuit quantum electrodynamics, *Rev. Mod. Phys.* **93**, 025005 (2021).
- [50] C. Wang, X. Li, H. Xu, Z. Li, J. Wang, Z. Yang, Z. Mi, X. Liang, T. Su, C. Yang *et al.*, Towards practical quantum computers: Transmon qubit with a lifetime approaching 0.5 milliseconds, *npj Quantum Inf.* **8**, 3 (2022).
- [51] C. W. Helstrom, *Quantum Detection and Estimation Theory* (Academic Press, New York, 1976).
- [52] See Supplemental Material at <http://link.aps.org/supplemental/10.1103/PhysRevLett.132.250204> for details on the experimental setup, theoretical calculations, experimental characterization, numerical simulations, and error analysis, which includes Refs. [53–56].
- [53] W. K. Wootters, Statistical distance and Hilbert space, *Phys. Rev. D* **23**, 357 (1981).
- [54] S. Pang and A. N. Jordan, Optimal adaptive control for quantum metrology with time-dependent Hamiltonians, *Nat. Commun.* **8**, 14695 (2017).
- [55] B. M. Escher, R. L. de Matos Filho, and L. Davidovich, General framework for estimating the ultimate precision limit in noisy quantum-enhanced metrology, *Nat. Phys.* **7**, 406 (2011).
- [56] S.-B. Zheng, One-step synthesis of multiatom Greenberger-Horne-Zeilinger states, *Phys. Rev. Lett.* **87**, 230404 (2001).
- [57] F. Motzoi, J. M. Gambetta, P. Rebentrost, and F. K. Wilhelm, Simple pulses for elimination of leakage in weakly nonlinear qubits, *Phys. Rev. Lett.* **103**, 110501 (2009).
- [58] J. M. Gambetta, F. Motzoi, S. T. Merkel, and F. K. Wilhelm, Analytic control methods for high-fidelity unitary operations in a weakly nonlinear oscillator, *Phys. Rev. A* **83**, 012308 (2011).
- [59] M. A. Nielsen and I. L. Chuang, *Quantum Computation and Quantum Information: 10th Anniversary Edition* (Cambridge University Press, Cambridge, England, 2010).
- [60] S. Boixo, S. V. Isakov, V. N. Smelyanskiy, R. Babbush, N. Ding, Z. Jiang, M. J. Bremner, J. M. Martinis, and H. Neven, Characterizing quantum supremacy in near-term devices, *Nat. Phys.* **14**, 595 (2018).
- [61] F. Arute, K. Arya, R. Babbush, D. Bacon, J. C. Bardin, R. Barends, R. Biswas, S. Boixo, F. G. S. L. Brandao, D. A. Buell *et al.*, Quantum supremacy using a programmable superconducting processor, *Nature (London)* **574**, 505 (2019).
- [62] S.-L. Zhu, Z.-D. Wang, and P. Zanardi, Geometric quantum computation and multiqubit entanglement with superconducting qubits inside a cavity, *Phys. Rev. Lett.* **94**, 100502 (2005).